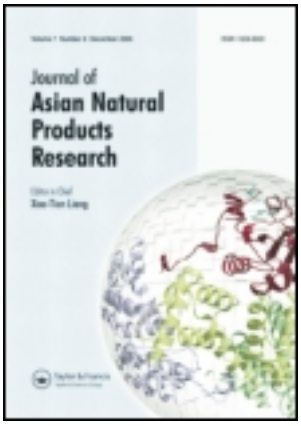

Journal of Asian Natural Products Research

Publication details, including instructions for authors and subscription information:
http://www.tandfonline.com/loi/ganp20

An *in vitro* transport model for rapid screening and predicting the permeability of candidate compounds at blood-brain barrier

Zhi-Hong Yang [a b], Xiao Sun [a], Chao Mei [a], Xiao-Bo Sun [a], Xiao-Dong Liu [b] & Qi Chang [a]

[a] Chinese Academy of Medical Sciences and Peking Union Medical College, Institute of Medicinal Plant Development, Beijing, 100193, China

[b] Key Laboratory of Drug Metabolism and Pharmacokinetics, China Pharmaceutical University, Nanjing, 210009, China

Available online: 25 Nov 2011

To cite this article: Zhi-Hong Yang, Xiao Sun, Chao Mei, Xiao-Bo Sun, Xiao-Dong Liu & Qi Chang (2011): An *in vitro* transport model for rapid screening and predicting the permeability of candidate compounds at blood-brain barrier, Journal of Asian Natural Products Research, 13:12, 1087-1097

To link to this article: http://dx.doi.org/10.1080/10286020.2011.599958

Journal of Asian Natural Products Research
Vol. 13, No. 12, December 2011, 1087–1097

An *in vitro* transport model for rapid screening and predicting the permeability of candidate compounds at blood–brain barrier

Zhi-Hong Yang[ab], Xiao Sun[a], Chao Mei[a], Xiao-Bo Sun[a]*, Xiao-Dong Liu[b]* and Qi Chang[a]

[a]*Chinese Academy of Medical Sciences and Peking Union Medical College, Institute of Medicinal Plant Development, Beijing 100193, China;* [b]*Key Laboratory of Drug Metabolism and Pharmacokinetics, China Pharmaceutical University, Nanjing 210009, China*

The aim of this study was to design and develop a simple *in vitro* blood–brain barrier (BBB) permeation model for elementarily and rapidly predicting the permeability of candidate compounds at BBB and further evaluating whether *P*-glycoprotein (*P*-gp) affects them across BBB. The model was mainly composed of cultured rat brain microvascular endothelial cells (rBMECs), glass contraption, and micropore membrane. First, we evaluated the model by morphological observation. Second, the restriction effects of paracellular transport were verified by measuring marker probes transport, and monitoring transendothelial electrical resistance (TEER) and leakage. Finally, protein expression and activity of *P*-gp were confirmed by carrying out Western blot analysis and polarized transport of rhodamine-123 (Rho123) in rBMECs. The rBMECs retained both endothelial cells and BBB features. The rBMECs model reproducibly attained approximately 130 $\Omega\,cm^2$ on the steady-state TEER value, and displayed a barrier function to marker probes transport by decreasing the permeability. Protein band of 170 kDa manifested the existence of *P*-gp in the rBMECs, and the findings of cyclosporin A-sensitive decrease of Rho123 efflux confirmed the presence of *P*-gp activity. A simple, rapid, and convenient *in vitro* BBB permeation model was successfully established and applied to evaluate the BBB transport profiles of three natural flavonoids: quercetin, naringenin, and rutin.

Keywords: permeation model; candidate compounds screening; blood–brain barrier; *P*-glycoprotein

1. Introduction

Owing to persistent high incidences, central nervous system (CNS) diseases rates are continuously increasing in Asia. Traditional herbal medicine is a plentiful and enormous treasure house of candidate compounds for preventing and treating CNS diseases. With more and more interest, screening candidate compounds with novel structure or efficacious action from herbal medicines is coming to be a realistic and promising treatment strategy for CNS diseases.

Passing through blood–brain barrier (BBB) is a prerequisite for treating CNS diseases. BBB is the main interface between the bloodstream and the brain parenchyma controlling the passage of endogenous and exogenous substrates into and out of the CNS. BBB is a selective and dynamic structure, and is mainly formed by brain microvascular endothelial cells (BMECs). *P*-glycoprotein (*P*-gp), the 170 kDa protein product of the multidrug resistance-1 (*MDR1*) gene, at brain, is mainly localized in the apical membrane of BMECs [1,2]. *P*-gp plays an important role in the integrity of BBB and protects the brain from many exogenous toxins.

*Corresponding authors. Email: xbsun@implad.ac.cn; lilikktom@tom.com

ISSN 1028-6020 print/ISSN 1477-2213 online

http://dx.doi.org/10.1080/10286020.2011.599958
http://www.tandfonline.com

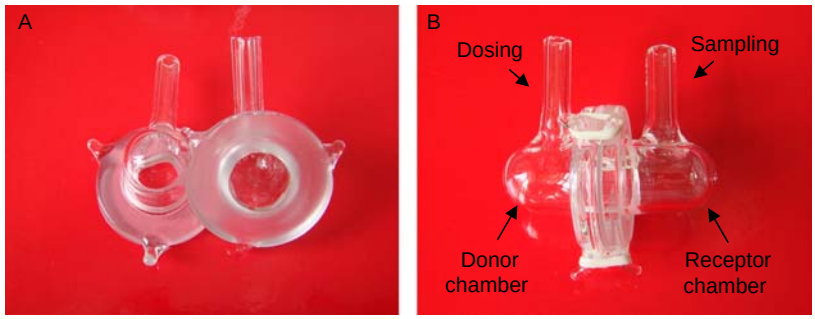

Figure 1. Photographs of the devised permeation apparatus.

P-gp effluxes a large number of structurally diverse chemotherapeutic agents [3–7], resulting in dramatically decreased pharmacological effects on the CNS to induce treatment failure [8–10]. So the permeability prediction of lead compounds, candidate drugs, or clinical drugs at BBB, and the further evaluation of the effects of *P*-gp on compounds across BBB are important and necessary.

In vitro cell screening experiment has major advantages, i.e. it is fast, it has low cost, it is fit for considerable samples, and its conditions are under control. There are some commercially available plate inserts in the market, but the cost, the less volume of added samples, and the disposable material impact their applications in the studies on a large number of compounds passing through the BBB. In this study, we design and develop a simple *in vitro* BBB transport model to elementarily and rapidly screen and predict the permeability of candidate or lead compounds at BBB and further evaluate whether *P*-gp affects them across BBB.

2. Results and discussion

2.1 Illustration of the novel permeation apparatus

The photographs of the novel permeation apparatus is shown in Figure 1. The schematic drawing of contrasting structures of *in vivo* BBB with *in vitro* model is described in Figure 2.

2.2 Morphology

Twelve days primary culture of endothelial cells achieved growth to a confluent

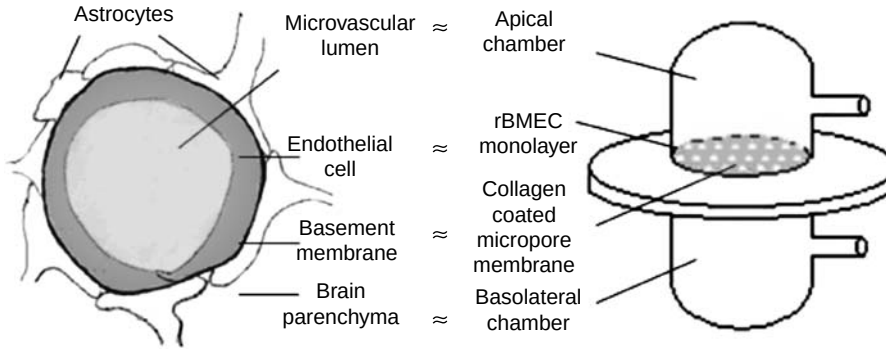

Figure 2. Schematic drawing of contrasting structures of *in vivo* BBB with *in vitro* model. The left panel showed a sketch of cross-section through a brain microvascular, which was surrounded by astrocyte endfeet. The right panel showed the experimental apparatus for transport studies.

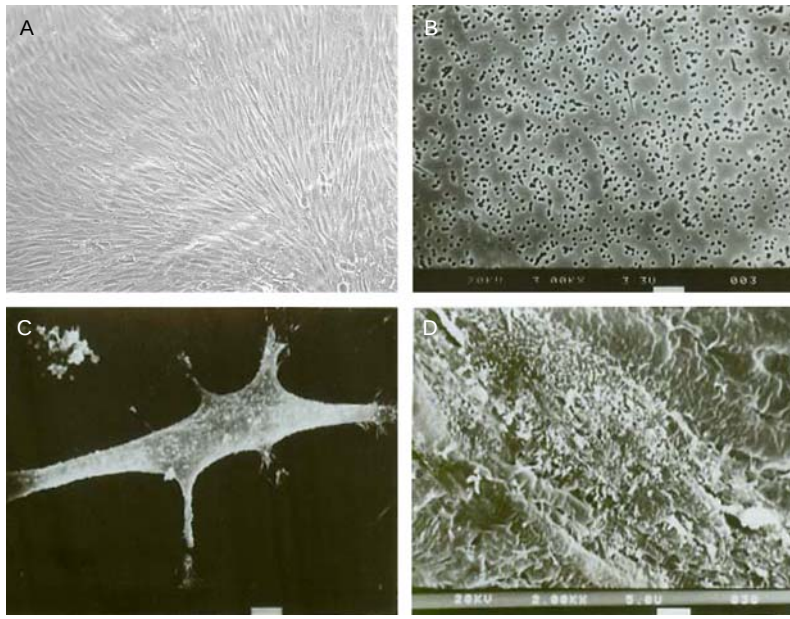

Figure 3. (A) Phase contrast photograph of a confluent primary passage rBMEC monolayer on 12 days primary culture (magnification 100 ×). (B) SEM photograph of blank micropore membrane with 0.4 μm pore size (2000 ×, bar = 3.3 μm). (C) SEM photograph of a single rBMEC (1500 ×, bar = 6.7 μm). Microvilli (white dots) covered the endothelial cell surface. (D) SEM photograph of a confluent rBMEC monolayer on the micropore membrane (2000 ×, bar = 5 μm).

monolayer with 20% newborn calf serum in the culture medium. Light microscopic image (100 ×) showed a characteristic elongate spindle-shaped morphology to the rat brain microvascular endothelial cells (rBMECs; Figure 3(A)). Scanning electron microscope (SEM) image showed the squamous morphology, i.e. microvilli (white dots) covered the endothelial cell surface (Figure 3(C)). At confluence, rBMECs formed a monolayer of small, tightly packed, nonoverlapping, contact-inhibited cells (Figure 3(D)). In these culture conditions, rBMECs retained the inherent features of both endothelial cell and BBB.

2.3 Bioelectric characteristics of rBMEC monolayer

Confluent rBMEC monolayer was grown on the Millicell-PCF insert. The transendothelial electrical resistance (TEER) values were measured from 4th to 24th days after seeding (Figure 4). The TEER increased to a peak value (above 130 Ω cm^2) at 15th day, and a plateau of TEER values was observed between 15th and 18th days. Following 18th day, the TEER values decreased slightly which were monitored until 24th day. The rBMECs model reproducibly attained approximately 130 Ω cm^2 on the steady-state TEER value at 15th day. Monolayer

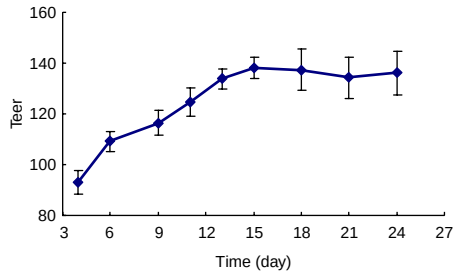

Figure 4. TEER values (Ω cm^2) of rBMECs on Millicell inserts between 4th and 24th days. Data were mean ± SD with $n = 8$ replicates.

Table 1. P_{app} and R of blank membranes and the cultured rBMEC monolayers to paracellular pathway transport markers, FLU, and FD-4.

In vitro BBB model	P_{app} ($\times 10^{-6}$ cm/s)		R (%)	
	FLU	FD-4	FLU	FD-4
Blank apparatus	54.4 ± 9.4	42.1 ± 5.9	38.4 ± 6.6	29.7 ± 4.2
rBMEC monolayer	7.2 ± 1.3**	2.8 ± 0.4**	5.1 ± 0.9**	2.0 ± 0.3**

Notes: Concentrations of FLU and FD-4 in apical chamber were set to be 1 and 100 μg/ml, respectively. At 3 h following transport, the concentrations of FLU and FD-4 in basolateral chamber were measured. Data were expressed as mean ± SD ($n = 4$; $^{**}p < 0.01$ vs. blank membranes).

with TEER value of more than 130 Ω cm^2 was used for experiment.

2.4 Leakage of rBMEC monolayer

Measurement of TEER is not always a restriction predictor of the paracellular pathway to substance transport [11]; therefore, the permeability of fluorescein (FLU, low-molecular weight 322 Da) and FITC-labeled dextran (FD-4, high-molecular weight 4 kDa), the markers for the predominantly paracellular pathway transport, was measured. The apparent permeability coefficients (P_{app}) of FLU and FD-4 across the empty micropore membranes were 54.4 ± 9.4 and 42.1 ± 5.9 (10^{-6} cm/s), respectively. However, in the presence of the rBMEC monolayers, the P_{app} of FLU and FD-4 decreased to 7.2 ± 1.3 and 2.8 ± 0.4 (10^{-6} cm/s), respectively. Moreover, the relative permeability ratio R was also notably decreased for FLU and FD-4 (Table 1). No significant differences of permeability to FLU and FD-4 between Millicell-PCF insert membrane group and Millipore polycarbonate membrane group were observed in the P_{app} values (50.5 ± 8.2 vs. 54.4 ± 9.4, 6.9 ± 1.4 vs. 7.2 ± 1.3, 43.7 ± 5.0 vs. 42.1 ± 5.9, 2.9 ± 0.2 vs. 2.8 ± 0.4; $p > 0.05$) [3]. Therefore, the monolayer model displayed a barrier function to substance transport as evidenced by decreased permeability compared with the permeability of the supporting membrane alone ($p < 0.01$).

2.5 P-*gp expression in cultured rBMECs*

The protein level of *P*-gp in the cultured rBMECs was detected by Western blot. The K562/A02 cells were served as positive control. The result revealed a band of 170 kDa, corresponding to *P*-gp (Figure 5). Similar staining intensities were found in three independent batches of the cultured rBMECs, manifesting the existence of *P*-gp in the cultured rBMECs.

2.6 Rhodamine-123 transport assay for P-*gp function*

To further assess the functional activity of *P*-gp in the cultured rBMECs, we measured the polarized transendothelial transport of rhodamine-123 (Rho123;

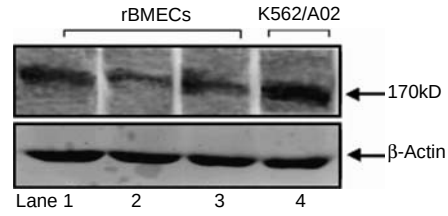

Figure 5. Western blot analysis of *P*-gp in the cultured rBMECs and K562/A02 cells. Protein preparations (20 μg) from the cultured rBMECs and K562/A02 cells were resolved on 8% SDS-polyacrylamide gel and electrophoretically transferred to a nitrocellulose membrane for successive blotting with anti-*P*-gp C219 and anti-β-actin antibody. Lanes 1–3 came from three independent batches of the cultured rBMECs.

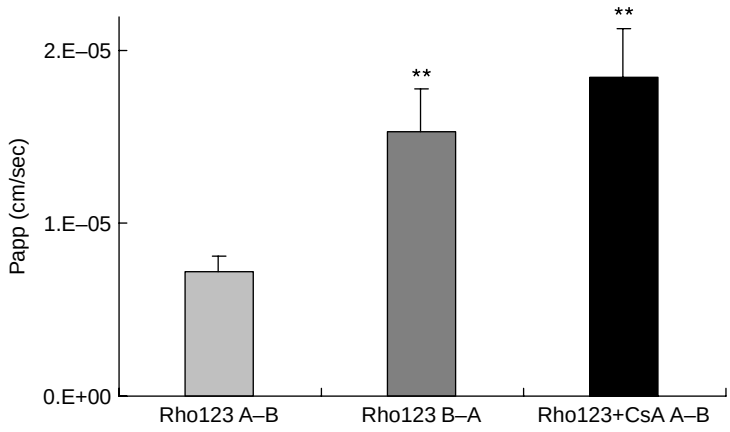

Figure 6. Rho123 transport across the cultured rBMEC monolayer. Polarized transport of Rho123 was undertaken in the A–B and B–A directions. Rho123 concentration was set to be 0.5 μM in donor chambers. Rho123 transport in the A–B direction was also measured in the presence of 50 μM CsA by adding to the A chambers. Mean ± SD ($n = 4$; $*p < 0.05$, $**p < 0.01$ vs. Rho123 A–B).

0.5 μM) in apical to basolateral (A–B) and basolateral to apical (B–A) directions either with or without *P*-gp inhibitor cyclosporin A (CsA; 50 μM). As shown in Figure 6, polarized transport of Rho123 in the rBMEC monolayer was found. Rho123 transport in the B–A direction was significantly greater than that in the A–B direction. The permeability of rBMEC monolayer to Rho123 in the B–A direction was 2.1-fold greater than that in the A–B direction at 120 min. Exposure of the monolayer to CsA (50 μM) significantly increased ($p < 0.05$) the permeability in the A–B direction to the values which were not notably different ($p > 0.05$) from the B–A data of Rho123 transport alone at the designed time. It indicated that the use of CsA almost inhibited *P*-gp-involved efflux mechanism presented in the rBMEC monolayer, resulting in an increase in P_{app} levels of 7.24×10^{-6} cm/s relative to that of 15.32×10^{-6} cm/s in A–B direction. These results were consistent with the observation that the *P*-gp-involved efflux occurs on the apical side, out of the cells.

2.7 Quercetin, naringenin, and rutin transport assay

The P_{app} levels of quercetin and naringenin were significantly more than that of rutin in the *in vitro* BBB model (Figure 7). Quercetin and naringenin transport in the B–A direction was greater than that in the A–B direction. The P_{app} values of quercetin, naringenin, and rutin across the rBMECs were 10.60 ± 1.41, 22.45 ± 3.32, and 0.08 ± 0.02 (10^{-6} cm/s), respectively, in the A–B direction. Moreover, in presence of CsA, the P_{app} values of quercetin and naringenin were increased to 16.83 ± 3.04 and 29.72 ± 4.13 (10^{-6} cm/s), respectively, in the A–B direction ($p < 0.05$). These data indicated that quercetin and naringenin could easily pass through the BBB, and *P*-gp might involve in the transport of them at the BBB. The entrance into brain of rutin might be limited by BBB.

2.8 Discussion

The passage of compounds and drugs from the blood into the CNS is restricted by the presence of the BBB, which separates and

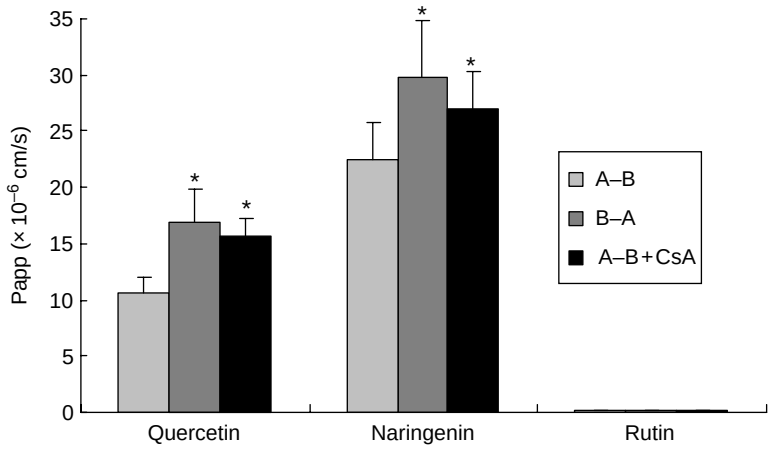

Figure 7. Quercetin, naringenin, and rutin transport across the cultured rBMEC monolayer. Polarized transport of quercetin and naringenin showed in the A–B and B–A directions. Three compound concentrations were set to be 50 μM in donor chambers. CsA concentration was set to be 50 μM by adding to the A chambers. Mean ± SD ($n = 4$; $*p < 0.05$, *vs*. control A–B).

isolates the microenvironment of the CNS. Because of the physical nature of BBB, transport across the barrier is generally dependent on the lipophilicity, molecular size, and protein complex formation of the compound. In addition, recent studies revealed that *P*-gp at BBB was thought to act as an active defense mechanism, restricting the penetration of a large number of structurally diverse drugs into the brain. The significant role of *P*-gp in defense against many lead compounds, candidate drugs, or clinical drugs by active efflux at BBB has been tightly relevant to drug resistance. With regard to drug efficacy, disposition, availability, metabolism, and drug–drug interactions, it is recognized that whether compound can pass through BBB and whether compound penetration is restricted by *P*-gp must be assessed properly before becoming a clinical drug.

The prediction of the property is important, but the experimental determination of BBB penetration *in vivo* is difficult and costly. So the purpose of our present study was to design and develop a simple, economical, and convenient *in vitro* transport model for elementarily and rapidly predicting the permeability of lead compounds, candidate drugs, or clinical drugs at BBB and further evaluating whether *P*-gp affects them across BBB.

As compared with some commercially available plate inserts in the market (Corning Costar, Millipore Millicell, etc.), the devised contraption was made by glass material. The model possesses the following major advantages: reusable, economical, environmental protection, convenient to be sterilized, stable for chemical agents and temperature, and more sample volume for bidirectional permeation experiments.

Nearly all components of BBB are the BMECs. So for studying the characteristics of drug transport across BBB, we used the cultured rBMECs as an *in vitro* BBB transport model. The functional assays of restriction of paracellular transport in the cultured rBMEC monolayer were evaluated by measuring FLU and FD-4 transport, and monitoring TEER and leakage. The functional activity of *P*-gp in the cultured rBMECs was confirmed by carrying out Rho123 transport in the cultured rBMEC monolayer. The

polarized transport of Rho123 revealed net greater transfer in the B–A direction across the cultured rBMECs monolayer. The transport of Rho123 in the B–A direction was 2.1-fold of that in the A–B direction at 120 min. Co-administration of CsA (50 μM) significantly increased ($p < 0.05$) the transport in the A–B direction. It demonstrated that the use of CsA almost inhibited *P*-gp-mediated efflux mechanism presented in the cultured rBMEC monolayer. It further manifested that the increased transport of Rho123 in rBMECs may be ascribed to the decreased *P*-gp functional activity by *P*-gp inhibitor. Even though CsA is not specific for *P*-gp, but also inhibited other transporters, such as MRP1, MRP2, and BCRP [12–14], it is often used as an inhibitor of *P*-gp in drug transport studies, especially in tissues, such as brain capillary endothelial cells. Moreover, MRP1 is not predominantly expressed in BBB [15,16]. Although the use of highly selective third generation *P*-gp inhibitor can give better understanding of *P*-gp-mediated transport of Rho123 at BBB, our results still manifested the findings of CsA-sensitive decrease in Rho123 efflux and confirmed the presence of *P*-gp activity in the cultured rBMECs. The results were in accordance with the preliminary Western blot analysis. All the results demonstrated that the cultured rBMEC monolayer remained both endothelial cell and BBB features including *P*-gp function.

Three natural flavonoids, such as quercetin, naringenin, and rutin, were tested by this *in vitro* model for evaluating the transport characteristics at BBB. Owing to the differences of lipophilicity and molecular size, the three compounds showed dissimilar profiling of BBB transport. Quercetin and naringenin showed polarized transport in the A–B and B–A directions, and could easily pass through the BBB. But the entrance of rutin into brain might be limited by BBB, and showed that rutin could hardly pass through the cultured rBMECs monolayer.

In conclusion, this study demonstrated that our *in vitro* BBB model represented a useful tool for elementarily and rapidly screening and predicting BBB permeability of candidate compounds, and it can be used to further evaluate whether *P*-gp affects these compounds across BBB and limits the efficacy of them in the CNS.

3. Experimental

3.1 Materials and agents

Micropore membranes (Isopore™, polycarbonate membrane, 0.4 μm pore-size) and Millicell-PCF inserts (1 cm diameter, 0.4 μm pore size) were purchased from Millipore Co. (Billerica, Massachusetts, USA). Bovine serum albumin (BSA) was purchased from SABC (Fraction V, Houston, TX, USA). Rho123, FLU, and FD-4 were purchased from Sigma Chemical Co. (St. Louis, MO, USA). CsA was provided by Sichuan Industrial Institute of Antibiotics (Chengdu, China).

P-gp monoclonal antibody (C219, IgG_{2a}) was purchased from Calbiochem of EMD Biosciences Inc. (Seattle, WA, USA), and polyclonal antibody IRDye 800-conjugated affinity purified anti-mouse IgG was purchased from Rockland Inc. (Rockland, Ontario, Canada). Blue-Ranger prestained protein molecular weight marker mix and polyclonal anti-β-actin antibody were purchased from Pierce Chemical Co. (Rockford, IL, USA) and Boster Biotech Co. (Wuhan, China), respectively. All other agents were commercially available.

3.2 Animals

Sprague–Dawley neonate rats, 7–10 days old, were supplied by the Center of Experimental Animals, China Pharmaceutical University. The studies were approved by the Animal Ethics Committee of China Pharmaceutical University.

3.3 Preparation of the permeation apparatus

To be conveniently sterilized and repetitively used, the apparatus was made of glass material. The volume of each part of the apparatus was about 1.2 ml, and the bottom area was 0.78 cm^2 (Figure 1(A)). In the transport experiment, the pretreated micropore membrane, on which BMECs achieved growth to a confluent monolayer, was fixed on the bottom side. Then the two parts of the apparatus were combined into one assembly unit (Figure 1(B)). The test agents were administered at the donor chamber, and samples were taken from the receptor chamber. The schematic drawing of *in vivo* BBB and *in vitro* BBB transport model is shown in Figure 2.

3.4 Preparation of culture surfaces

For coating of the micropore membranes, we diluted the self-prepared Richmond, rat-tail collagen stock solution with sterile deionized water to a final protein concentration of 50 μg/ml [17]. Approximately, 40 μl of this freshly prepared solution was applied to per cm^2 of membrane surface and dried at room temperature. No further washing steps were carried before plating the cells. Coated surfaces can be stored dry at room temperature for several weeks.

3.5 rBMECs isolation and primary culture

A most important component of BBB is the BMEC. So for studying the characteristics of compounds transport across BBB, we used the cultured rBMECs as an *in vitro* BBB transport model. The cell isolation and culture were operated according to the previous method done in our laboratory [3,18,19]. Briefly, freshly isolated rBMECs were cultured for 10–12 days in 2% gelatin-precoated tissue flasks for a primary passage cell growth, then plated onto either micropore membranes or Millicell-PCF inserts at a seeding density of 1×10^5 cells/cm^2. Cultures were under the normal cell culture conditions, maintained in a humidified atmosphere (5% CO_2/95% air) at 37°C with a medium comprising DME/F-12 1:1 (Hyclone, Logan, UT, USA) supplemented with 20% newborn calf serum (Gibco, Invitrogen Corporation, Auckland, New Zealand), L-glutamine (0.9 g/l), heparin (50 mg/l), streptomycin (105 U/ml), penicillin (105 U/ml), and $NaHCO_3$ (1.2 g/l), pH 7.2. Culture medium was replaced every 3 days. Identification of at least 95% of cell population as brain endothelial cells was based on the positive staining with an antibody against Factor VIII-related antigen [20].

3.6 Detection of P-gp expression by Western blot

Western blot was used for investigating the expression of *P*-gp in the cultured rBMECs. Briefly, the cultured rBMECs were collected and homogenized in ice-cold cell lysis containing 10 mM Tris–HCl, 1 mM $MgCl_2 \cdot 6H_2O$, 1 mM EGTA, 1 mM mercaptoethanol, 1% glycerin, and protease inhibitor cocktail (1 mM dithiothreitol, 2 mM phenylmethylsulfonylfluoride) (Sigma Chemical Co., St. Louis, MO, USA). Then the homogenate was centrifuged at 11,000 rpm for 10 min at 4°C. The supernatant was obtained as membrane fractions for Western blot, and the protein concentration in this solution was measured with a Bio-Rad Protein Assay (Bio-Rad Laboratories, CA, USA) using BSA as a standard. An aliquot of cell sample was diluted with a volume of 4 × SDS sample buffer containing 0.1 M tris–HCl, 4% SDS, 200 mM DDT, 20% glycerin, and 0.2% bromophenol blue. The protein (20 μg) was separated by electrophoresis on 8% SDS-polyacrylamide gel and electrophoretically transferred to a nitrocellulose membrane (BioTrace NT, PallCor, Ann Arbor, MI, USA). The membrane was blocked by PBS containing 0.1% Tween-20 (PBST) and 5% dried

skim milk at room temperature for 1 h and rinsed three times for 15 min in PBST. Then the membrane was incubated with the primary monoclonal antibody C219, diluted 200-fold in PBST, overnight at 4°C. After being rinsed with PBST, the membrane was incubated with the secondary polyclonal antibody IRDye 800-conjugated affinity-purified anti-mouse IgG diluted 12,000-fold in PBST at room temperature for 1 h. Detection was carried out by the Odyssey Infrared Imaging System (LI-COR Inc., Lincoln, Nebraska, USA). All blots were stripped and reprobed with polyclonal anti-β-actin antibody to ascertain equal loading of protein.

3.7 Ultrastructural morphology of rBMECs

The rBMECs were fixed at room temperature for 1 h with glutaraldehyde (2.5% v/v) and paraformaldehyde (4% v/v) in phosphate buffer, and postfixed in osmium tetroxide (1% w/v) for 1 h. After dehydrating in acetone and critical point drying, the cells were sputtered with gold (50 nm) in a Balzers Union sputtering machine and observed in an AKASHI SX-40 SEM.

3.8 TEER measurement

Restriction of paracellular transport of small ions was determined by the analysis of TEER. rBMECs were cultured on Millicell-PCF inserts. For each insert, the electrical resistance was measured by an EVOMX-A voltmeter (World precision instruments Inc., Sarasota, Florida, USA). TEER ($\Omega\,cm^2$) was calculated from the displayed electrical resistance on the readout screen and a correction for insert surface area was made.

3.9 Permeability assessment

Assessment of the 3 h permeability of rBMEC monolayer to the paracellular pathway transport markers, FLU and FD-4, was undertaken at day 15 post-seeding in Millicell-PCF inserts and micropore membranes. Briefly, at 15 min before the start of the experiment, inserts and membranes were removed to empty the wells within a cell culture plate and the apical and basolateral chambers fed with pH 7.4 Hanks' balanced salt solution (HBSS, pre-warmed to 37°C). After the incubation, the solution was removed and replaced with HBSS containing 1 μg/ml FLU or 100 μg/ml FD-4 at the start of the experiment to the apical chamber. After 3 h, the concentration of FLU and FD-4 in the basolateral chamber was determined by HPLC and fluorescence spectrophotometer, respectively. Paracellular transports of FLU and FD-4 across rBMEC monolayers on the blank supporting membranes of the assembled apparatus were carried out with the similar operation. The P_{app} and R values for both markers were calculated according to the following equations [21]:

$$P_{app} = \left(\frac{V_{acceptor}}{\text{Area} \times \text{time}}\right) \times \frac{C_{acceptor}}{C_{inital,donor}},$$

$$R = \frac{C_{3,acceptor}}{C_{initial,donor}} \times 100\%.$$

3.10 Polarized Rho123 transport on the model

Transport assay of Rho123, the typical substance for *P*-gp as previously described [12,22,23], was used to assess the functional activity of *P*-gp in the cultured rBMECs. The polarized transendothelial transports of Rho123 (0.5 μM) in the A–B and B–A directions either with or without *P*-gp modulator CsA (50 μM) were investigated. Briefly, rBMECs were cultured on micropore membranes for 15 days after seeding. At 15 min before to the start of the experiment, the membranes were

removed to empty the wells within a cell culture plate and incubated with pH 7.4 HBSS (37°C). Then the solution was removed, and the membranes were fixed into the assembled apparatus. The transport experiments in A–B or B–A direction were initiated by adding 1.2 ml Rho123 (0.5 μM) to donor chamber (A or B chamber), and another chamber was filled with equal volume of HBSS. At 120 min, 50 μl samples were taken from the acceptor chamber (B or A chamber) with replenishment by fresh HBSS. The transports of Rho123 in the presence or absence of CsA (50 μM) were measured at 37°C periodically for 120 min, and the modulator CsA was added to the A chamber. Each transport group consisted of four replicates, with each study repeated twice. The P_{app} for Rho123 was calculated according to the equation mentioned above.

3.11 Model application

The transendothelial transports of quercetin, naringenin, and rutin in bilateral directions either with or without CsA were investigated. The cell culture, drug administration, and sampling were operated similar to the method in Section 3.10. The transports of quercetin (50 μM), naringenin (50 μM), and rutin (50 μM) in the presence or absence of CsA (50 μM) were measured at 37°C periodically for 120 min. Each transport group consisted of four replicates, with each study repeated twice. The P_{app} values of quercetin, naringenin, and rutin were calculated.

3.12 Statistical analysis

All values were expressed as mean ± SD. Statistical analysis was accomplished using Student's *t*-test. A *p*-value less than 0.05 or 0.01 was considered statistically significant.

Acknowledgements

This work was supported by the National Science and Technology Specific Project of China (Nos 2009ZX09301-003 and 2009ZX09502-015), Research Fund for the Doctoral Program of Higher Education of China (No. 20101106120049), and Key Project of the National Eleventh Five-Year Research Program of China (No. 2008BAI51BOO).

References

[1] H. Sun, H. Dai, N. Shaik, and W.F. Elmquist, *Adv. Drug Deliv. Rev.* **55**, 83 (2003).
[2] H. Kusuhara and Y. Sugiyama, *Drug Discov. Today* **6**, 150 (2001).
[3] Z.H. Yang and X.D. Liu, *Epilepsy Res.* **78**, 40 (2008).
[4] H. Potschka, M. Fedrowitz, and W. Löscher, *Neuroreport* **12**, 3557 (2001).
[5] H. Potschka and W. Löscher, *Neuroreport* **12**, 2387 (2001).
[6] W. Löscher and H. Potschka, *NeuroRx* **2**, 86 (2005).
[7] A.H. Schinkel and J.W. Jonker, *Adv. Drug Deliv. Rev.* **55**, 3 (2003).
[8] H. Kubota, H. Ishihara, T. Langmann, G. Schmitz, B. Stieger, H.G. Wieser, Y. Yonekawa, and K. Frei, *Epilepsy Res.* **68**, 213 (2006).
[9] P. Kwan and M.J. Brodie, *Epilepsia* **46**, 224 (2005).
[10] P. Kwan, G.J. Sills, B.S. Meldrum, E.C. de Lange, T.W. Gant, E. Butler, G. Forrest, and M.J. Brodie, *Epilepsia* **41**(Suppl. 7), 161 (2000).
[11] T. Mukherjee, E. Squillantea, M. Gillespieb, and J. Shao, *Drug Deliv.* **11**, 11 (2004).
[12] R. Yumoto, T. Murakami, Y. Nakamoto, R. Hasegawa, J. Nagai, and M. Takano, *J. Pharmacol. Exp. Ther.* **289**, 149 (1999).
[13] Z.S. Chen, T. Kawabe, M. Ono, S. Aoki, T. Sumizawa, T. Furukawa, T. Uchiumi, M. Wada, M. Kuwano, and S.I. Akiyama, *Mol. Pharmacol.* **56**, 1219 (1999).
[14] M. Qadir, K.L. O'Loughlin, S.M. Fricke, N.A. Williamson, W.R. Greco, H. Minderman, and M.R. Baer, *Clin. Cancer Res.* **11**, 2320 (2005).
[15] P.M. Gerk and M. Vor, *J. Pharmacol. Exp. Ther.* **302**, 407 (2002).
[16] W. Löscher and H. Potschka, *J. Pharmacol. Exp. Ther.* **301**, 7 (2002).
[17] H. Franke, H. Galla, and C.T. Beuckmann, *Brain Res. Protoc.* **5**, 248 (2000).

[18] L. Zhang, X.D. Liu, L. Xie, and G.J. Wang, *Acta Pharmacol. Sin.* **24**, 903 (2003).
[19] J.J. Sun, L. Xie, and X.D. Liu, *Acta Pharmacol. Sin.* **27**, 249 (2006).
[20] Z.Y. Qian, Q. Huang, L.Y. Zhou, and Z.F. Sun, *Chin. J. Cell Biol.* **21**, 42 (1999).
[21] P. Artursson, *J. Pharm. Sci.* **9**, 476 (1990).
[22] J.S. Lee, K. Paull, M. Alvarez, C. Hose, A. Monks, M. Grever, A.T. Fojo, and S.E. Bates, *Mol. Pharmacol.* **46**, 627 (1994).
[3] M. Fontaine, W.F. Elmquist, and D.W. Miller, *Life Sci.* **59**, 1521 (1996).